Heterogeneous Catalysis

DOI: 10.1002/ange.201007484

The Mechanism of Potassium Promoter: Enhancing the Stability of Active Surfaces**

Chun-Fang Huo, Bao-Shan Wu, Peng Gao, Yong Yang, Yong-Wang Li, and Haijun Jiao**

Owing to their outstanding effect on improving catalytic reactivity, alkali-metal promoters have been widely used in industry[1,2] and extensively studied in academia.[3–12] Potassium-promoted iron catalysts for Fischer–Tropsch synthesis (FTS) and ammonia synthesis are the most representative examples of this effect. Owing to the complexity of real catalytic systems, the microscopic understanding of the alkali-metal promotion effect is still an elusive and challenging subject.

In the past decades, most experimental and theoretical studies have focused on the co-adsorption systems involving alkali-metal atoms, for example, K + CO/metal. Five types of alkali-metal–adsorbate interactions were proposed to explain the alkali-metal promotion effect: 1) substrate-mediated charge transfers,[3] 2) direct bonding between alkali metal and adsorbate,[4] 3) electrostatic interactions,[5] 4) alkali-metal-induced molecular polarization,[6] and 5) nonlocal alkali-metal-induced enhancement of the surface electronic polarizability.[7] Although these studies represent excellent surface science, they are not immediately relevant to catalysis, because alkali-metal salts (or oxides) rather than metallic alkalis are used in heterogeneous catalysis. More importantly, previous studies only highlighted the alkali-metal-induced effect on the electronic structure of metallic substrate and co-adsorbed molecules, while the more intriguing aspect, the alkali-metal effect on the surface structure of catalysts, has never been taken into account. On the basis of these proposals, the drastic changes in catalytic activity and selectivity caused by very low loadings of alkali-metal promoters cannot be reasonably explained.[8]

As metallic iron is the active catalyst in ammonia synthesis,[9] iron-based FTS catalysts show an rich phase chemistry of metal, oxides, and carbides under reaction conditions.[10] Since α-Fe is active in N_2/CO dissociation and hydrogenation, we take K_2O/Fe as a model catalyst to explore the morphology control effect theoretically and experimentally. It is found that one crucial effect of the potassium promoter is to modify the crystallographic orientation in favor of the formation of crystallites with abundant highly active facets.

Potassium promoter is usually added to the catalyst precursor by impregnation with potassium salt solution (K_2CO_3, $KHCO_3$, KNO_3 or KOH). During calcination and reduction, K_2O is formed and tends to segregate on the catalyst surface. However, no X-ray diffraction peaks of crystalline K_2O were detected in fresh and reduced catalysts,[11] thus indicating high K_2O dispersion. By studying the interaction of potassium and oxygen with iron surfaces, Pirug et al. observed an order c(4×2) co-adsorption structure on Fe(110) for strong K–O interaction (with c(4×2) representing potassium and oxygen co-adsorption on Fe(110) resulting in a diperiodic surface structure, which has a centered unit mesh with the surface vectors parallel to, but four and two times as long as the corresponding basic vectors of Fe(110)),[12] and Paál et al. further suggested that the composite Fe-O-K layer is the actual surface phase of working catalysts instead of bulk K_2O.[9] These studies validate molecular K_2O as a reasonable model to explore the promotion effect on Fe surfaces.

Morphology control of small particles, which is very important in heterogeneous catalysis, provides diverse surface structures with specific atomic arrangements by changing the crystallographic orientation.[13] Figure 1 shows the structures of seven typical body-centered cubic (bcc) Fe facets and the possible sites for K_2O adsorption. The low-index (110), (100), and (111) facets represent the basic structures of bcc Fe surfaces, that is, (110) is the closest-packed flat surface, (100) is relatively open with an atomic arrangement in fourfold symmetry, and (111) is a very open kinked surface with the second- and third-layer atoms exposed to the surface. The high-index facets are stepped or kinked surfaces and exhibit terrace-step structure with atomic arrangements similar to (110) or (100). For example, (211) and (321) can be considered as a monatomic stepped (110) surface with a terrace in one or two atomic widths. For (310) and (210), the (110)-like terrace is separated by a monatomic step of (100) symmetry leading to the step atoms with kink features. As a result, different performances for K_2O adsorption on these crystal facets can be expected.

To avoid direct interaction between K_2O molecules in adjacent unit cells, all adsorption sites have been examined on supercell slab models in Figure 1. The optimized structures, key bond parameters, and adsorption energies (E_{ads}) are given in Supporting Information Figure S1 and Table S1. It is found that K_2O adsorbs on the Fe surfaces through both O^{2-} and K^+, forming a bent geometry with Fe–O, Fe–K, and K–O

[*] Dr. C.-F. Huo, Dr. B.-S. Wu, Dr. P. Gao, Dr. Y. Yang, Dr. Y.-W. Li, Dr. H. Jiao
State Key Laboratory of Coal Conversion
Institute of Coal Chemistry, Chinese Academy of Sciences
and
Synfuels China Co., Ltd., Taiyuan, Shanxi (P. R. China)
E-mail: hcf905@sxicc.ac.cn
Dr. H. Jiao
Leibniz-Institut für Katalyse e.V. an der Universität Rostock
Albert-Einstein-Strasse 29a, 18059 Rostock (Germany)
E-mail: haijun.jiao@catalysis.de

[**] We thank the National Natural Science Foundation of China (No. 20873173) and National Outstanding Young Scientists Foundation of China (No. 20625620, Y.-W.L.) for financial support.

Supporting information for this article is available on the WWW under http://dx.doi.org/10.1002/anie.201007484.

© 2011 Wiley-VCH Verlag GmbH & Co. KGaA, Weinheim

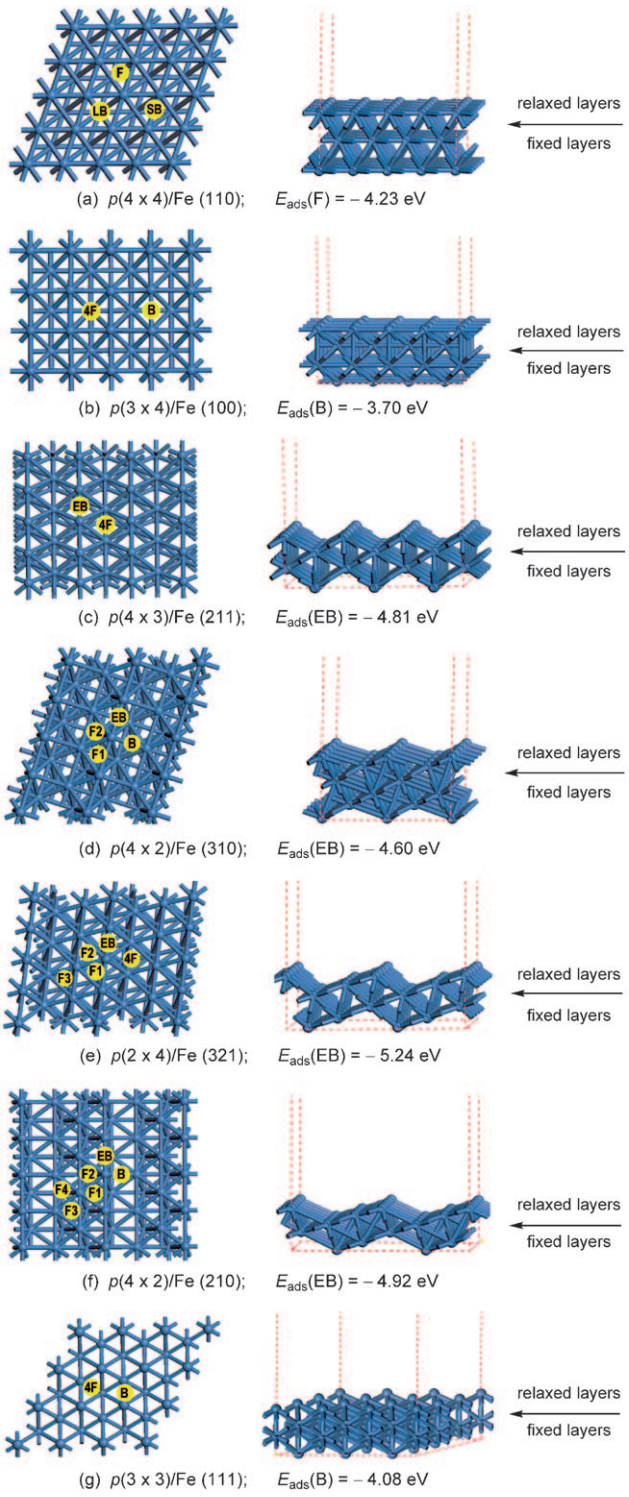

Figure 1. Top and side views of Fe(110), (100), (211), (310), (321), (210), and (111) as well as the possible adsorption sites (yellow) and the largest adsorption energy for K_2O adsorption on each surface. Abbreviations represent threefold sites (F, F1, F2, F3, and F4), bridge sites (B), long-bridge sites (LB), short-bridge sites (SB), fourfold sites (4F) and edge-bridge (EB) sites. $p(q\times r)$ indicates a superstructure with q and r multiples of the smallest repeat unit along the corresponding surface vectors, respectively.

distances in the range of 1.851–2.204, 2.766–3.407, and 2.515–3.090 Å, respectively. K_2O adsorption on the Fe surfaces is highly exothermic, and the most stable adsorption site and energy depend on the crystallographic orientation (Figure 1). On (110) and (100) surfaces, K_2O prefers to adsorb at the threefold (F) site and the bridge (B) site with adsorption energies of −4.23 and −3.70 eV, respectively. On (211), (310), (321) and (210) surfaces, O^{2-} tends to occupy the edge-bridge (EB) site, and the adsorption energies are −4.81, −4.60, −5.24, and −4.92 eV, respectively. Detailed comparison of adsorption energy of different crystal facets shows that three surface structures favor K_2O adsorption: 1) terrace-step structure, 2) terrace in two atomic widths, and 3) (110)-like structure. Since K_2O mainly adsorbs on the most stable site at low coverage, the K_2O adsorption energy has the order of (321) > (210) > (211) > (310) > (110) > (111) > (100). This result indicates that K_2O adsorption can stabilize the Fe crystal facets to different degrees.

To reveal the stabilization effect of K_2O clearly, we calculated the surface energy of seven facets with different K/Fe atomic ratios. For clean surfaces without K_2O, the surface energy is determined by $E_{surf,0} = (E_{slab} - N E_{bulk})/2A_0$, where E_{slab} and E_{bulk} are the total energies of the slab and one bulk unit cell, respectively, N is the number of bulk units in the slab, and A_0 is the surface area of the slab. For surfaces with low K_2O converge, the surface energy can be evaluated by $E_{surf} = E_{surf,0} + m E_{ads}/A$, where $m E_{ads}/A$ represents the change of the surface energy caused by K_2O deposition, m is the number of K_2O molecule on the substrate, and A is the surface area of the substrate. According to this definition, the lower the surface energy, the more stable the surface structure.

As shown in Table 1, our computed surface energies for clean Fe crystal facets agree well with the calculated values by Błoński and Kiejn[14] and the experimental estimation for a polycrystalline surface (2.41 $J m^{-2}$).[15] From the variation curves in Figure 2, we can see that as the surface K/Fe atomic ratio increases, all surface energies decrease, and all facets become more stable. Among them, (211) and (321) have the strongest increase in stability, while the weakest increase is found for (100). Hence, the relative stability of crystal facets can be altered upon K_2O coverage. For clean Fe surfaces, the relative stability has the order of (110) > (100) > (310) ≈ (211) > (321) > (210) > (111). At K/Fe ratios larger than 1/48, (211) and (310) become more stable than (100). When the K/Fe ratio increases to 1/12, (211) and (321) are even more stable than (110).

Table 1: Surface energies (E_{surf}, $J m^{-2}$) for the Fe(*hkl*)–K_2O system.

K/Fe	0	1/96	1/48	1/24	1/12
(110)	2.37 (2.37)[a]	2.31	2.25	2.13	1.88
(100)	2.44 (2.47)[a]	2.40	2.36	2.29	2.14
(211)	2.49 (2.50)[a]	2.41	2.33	2.17	1.85
(310)	2.48 (2.53)[a]	2.42	2.36	2.24	2.00
(321)	2.56 (2.59)[a]	2.47	2.39	2.22	1.87
(210)	2.58 (2.60)[a]	2.52	2.45	2.31	2.05
(111)	2.60 (2.58)[a]	2.53	2.45	2.31	2.02

[a] Values in parentheses are taken from reference [14].

© 2011 Wiley-VCH Verlag GmbH & Co. KGaA, Weinheim

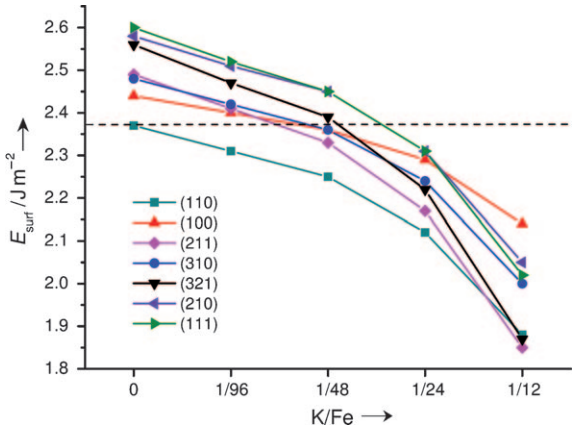

Figure 2. Surface energy variation versus the surface atomic ratio of K to Fe.

Generally, active crystal facets with large surface energy will shrink or even diminish rapidly during the crystal growth process as a result of minimizing surface energy of small crystallite. Therefore, enhancing the relative stability of the active surfaces is essential for designing catalysts with high activity and selectivity. It should also be pointed out that the contribution of a crystal facet to exposed surface area depends not only on its surface energy but also on its orientation.[16] To verify this point, the equilibrium shapes of small Fe crystallites at K/Fe = 0, 1/48, and 1/12 have been obtained from Wulff construction on the basis of the computed surface energies. Owing to their close normal directions and larger surface energies in comparison with (211) and (310), the facets (321) and (210) do not appear on the equilibrium-morphology crystallites (Figure 3). According to Wulff construction, the thermodynamically most stable (110) facet has the largest contribution to the total surface area of the clean Fe crystallite with a percentage of 39%, followed by (211) (32%), (310) (22%), and (100) (6%). During the course of the crystal growth, the expansion of (211) is competitive to (110) and (310), as is that of (310) to (100). Therefore, lowering the surface-energy differences between these competitive facets by K_2O loading will increase the proportion of (211) and (310). As the K_2O loading reaches K/Fe = 1/48, for example, the percentages of (211) and (310) increase from 32 and 22% to 35 and 31%, respectively. In particular, upon K/Fe to 1/12, (211) becomes the predominantly exposed facet covering about 70% of the total surface area; meanwhile, the (110) surface area sharply drops to 20%.

This modification effect of K_2O on the crystallographic orientation of α-Fe has been confirmed by transmission electron microscopy (TEM) and X-ray diffraction (XRD) of the H_2-reduced Fe/K catalysts. By means of TEM, we have examined the crystallographic nature of the system. The catalyst without K_2O mainly exposes its (110) facet with a *d* spacing of 0.203 nm (Figure 4a). In comparison, a large amount of (211) facet was observed on the catalyst with K/Fe ratio of 0.031, as indicated by a *d* spacing of 0.117 nm (Figure 4b). To gain further insight, an approximately quantitative analysis has been performed on the basis of XRD patterns (Figure 4). As we know, the diffraction intensity is generally described as given in Equation (1):

$$I = K L_P |F_{hkl}|^2 P e^{-2M} A(\theta) \quad (1)$$

where K is a constant for a particular experimental setup, L_P is the diffraction angle factor, which can be expressed as given

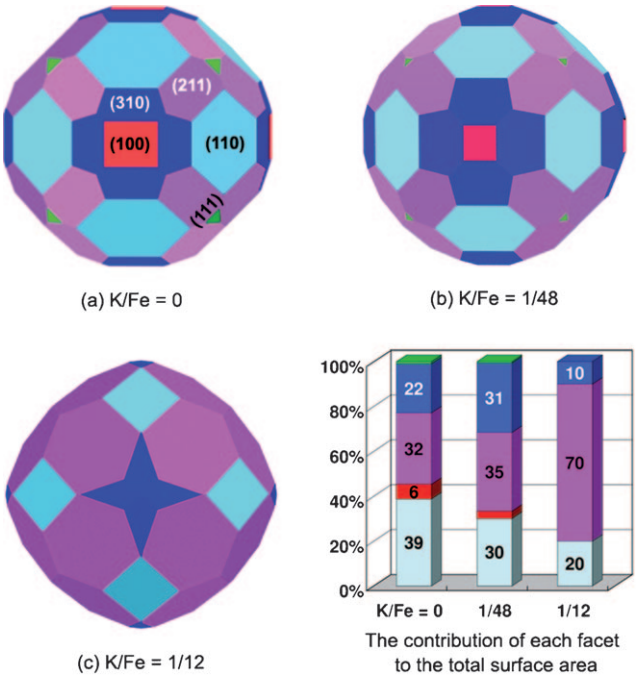

Figure 3. Equilibrium shapes of the small Fe crystallites obtained by Wulff construction.

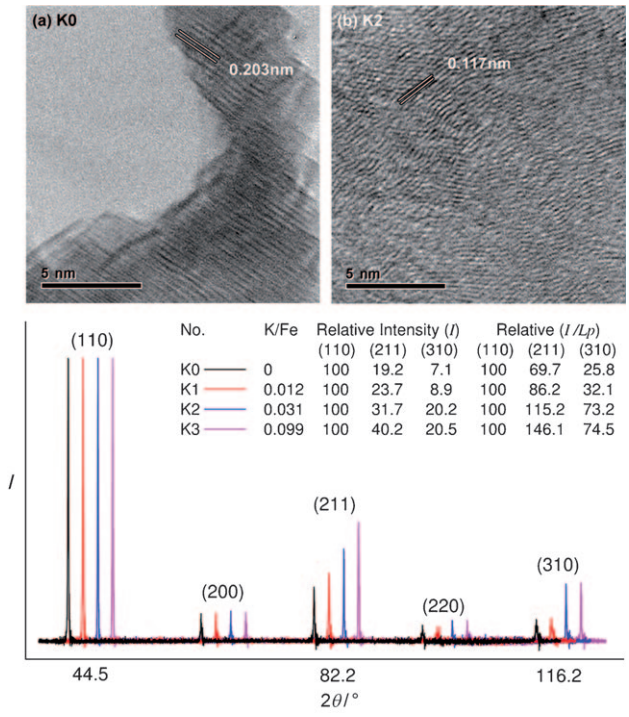

Figure 4. a,b) TEM images and c) XRD patterns (bottom) of the model Fe catalysts after H_2 reduction.

© 2011 Wiley-VCH Verlag GmbH & Co. KGaA, Weinheim

in Equation (2):

$$L_P = (1+\cos^2 2\theta)/(\sin^2\theta\cos\theta) \quad (2)$$

and F_{hkl} is the structure factor. For bcc Fe, when $h+k+l$ is even, $F_{hkl}=2f_{Fe}$; when $h+k+l$ is odd, $F_{hkl}=0$. P is the multiplicity factor of reflection hkl, which depends on the numbers of facets, e^{-2M} is the temperature factor, and $A(\theta)$ is the absorption factor, for a planar sample, which has no relation to the diffraction angle θ.

Therefore, the relative numbers of bcc Fe crystal facets can be estimated by the relative I/L_P values of diffraction peaks. From data in Figure 4, we can see that as the catalyst surface K/Fe ratio rises, the proportions of (211) and (310) to (110) increase. For example, when K/Fe = 0.031, the relative numbers of (211) and (310) to (110) have increased from 69.7:100 and 25.8:100 to 115.2:100 and 73.2:100. It is noteworthy that (211) and (310) have a high density of atomic steps. The low-coordinate atoms at these steps can strongly interact with reactant molecules and serve as active sites for activating chemical bonds.[17] As a consequence, the catalytic activity is enhanced dramatically.

In conclusion, our theoretical and experimental studies reveal that potassium promoter (K_2O) can stabilize the high-index and much more active facets such as Fe(211) and Fe(310) to be the energetically favored facets. This stabilizing effect changes the relative rate of crystal growth in different directions, which facilitates the formation of small particles with a large percentage of more active facets. This finding opens a new perspective for understanding the promotion effect and provides an innovative idea for designing efficient catalysts with controllable surface structures.

Experimental Section

Computations: All spin-polarized density functional theory calculations were carried out using Perdew–Burke–Ernzerhof (PBE) functional[18] and projector augmented wave (PAW) potentials,[19] as implemented in the VASP code.[20] The cutoff energy was set to 400 eV. For getting the well-converged surface energies of clean facets, more than 13-layer $p(1\times1)$ slab models with inversion symmetry[14] were fully optimized with $10\times10\times1$, $9\times9\times1$, $10\times6\times1$, $6\times6\times1$, $4\times10\times1$, $9\times4\times1$, and $7\times7\times1$ k point sampling for (110), (100), (211), (310), (321), (210), and (111), respectively. For K_2O adsorption calculations, a k-point mesh of $5\times5\times1$ was adopted. Moreover, dipole corrections are essential for obtaining reasonable K_2O adsorption energy.

Experiments: The model Fe catalyst was prepared by precipitation of Fe nitrate with aqueous ammonia at pH 8.5–9.0. The precipitate was filtered, washed thoroughly with deionized water, and spray dried at 250 °C. Potassium was introduced by impregnation with $KHCO_3$ solution before calcination at 400 °C. The oxidized precursor was reduced at 400 °C for 30 h under pure H_2 atmosphere and subsequently quickly quenched and passivated in 0.5 % O_2/He gas mixture. The reduced sample was suspended in ethanol for structural characterization. TEM images were recorded on a GEM-2010 microscope. The XRD measurements were carried out using a Rigaku D/max −2500 powder X-ray diffractometer with $Cu_{K\alpha}$ radiation ($\lambda = 0.154$ nm).

Received: November 29, 2010
Revised: March 1, 2011
Published online: June 28, 2011

Keywords: oxides · crystallographic orientation · heterogeneous catalysis · potassium · promotion effect

[1] "Promoters and Poisons": B. E. Koel, J. Kim in *Handbook of Heterogeneous Catalysis*, *Vol. 3* (Eds.: G. Ertl, H. Knözinger, F. Schüth, J. Weitkamp), Wiley-VCH, Weinheim, **2008**, p. 1593.
[2] W.-D. Mross, *Catal. Rev. Sci. Eng.* **1983**, *25*, 591 – 637.
[3] a) E. Wimmer, C. L. Fu, A. J. Freeman, *Phys. Rev. Lett.* **1985**, *55*, 2618 – 2621; b) D. C. Sorescu, *Surf. Sci.* **2011**, *605*, 401 – 414.
[4] Z. P. Liu, P. Hu, *J. Am. Chem. Soc.* **2001**, *123*, 12596 – 12604.
[5] J. J. Mortensen, B. Hammer, J. K. Norskov, *Phys. Rev. Lett.* **1998**, *80*, 4333 – 4336.
[6] S. J. Jenkins, D. A. King, *J. Am. Chem. Soc.* **2000**, *122*, 10610 – 10614.
[7] T. S. Rahman, S. Stolbov, F. Mehmood, *Appl. Phys. A* **2007**, *87*, 367 – 374.
[8] A. P. Raje, R. J. O'Brien, B. H. Davis, *J. Catal.* **2008**, *260*, 7 – 16.
[9] Z. Paál, G. Ertl, S. B. Lee, *Appl. Surf. Sci.* **1981**, *8*, 231 – 249.
[10] a) R. A. Dictor, A. T. Bell, *J. Catal.* **1986**, *97*, 121 – 136; b) E. de Smit, F. Cinquini, A. M. Beale, O. V. Safonova, W. van Beek, P. Sautet, B. M. Weckhuysen, *J. Am. Chem. Soc.* **2010**, *132*, 14928 – 14941.
[11] a) Y, Yang, H.-W. Xiang, Y.-Y. Xu, L. Bai, Y.-W. Li, *Appl. Catal. A* **2004**, *266*, 181 – 194; b) G. Connell, J. A. Dumesic, *J. Catal.* **1985**, *92*, 17 – 24.
[12] G. Pirug, G. Brodén, H. P. Bonzel, *Surf. Sci.* **1980**, *94*, 323 – 338.
[13] a) X. Xie, Y. Li, Z.-Q. Liu, M. Haruta, W. Shen, *Nature* **2009**, *458*, 746 – 749; b) C. Burda, X. B. Chen, R. Narayanan, M. A. El-Sayed, *Chem. Rev.* **2005**, *105*, 1025 – 1102.
[14] P. Błoński, A. Kiejn, *Surf. Sci.* **2007**, *601*, 123 – 133.
[15] W. R. Tyson, W. A. Miller, *Surf. Sci.* **1977**, *62*, 267 – 276.
[16] G. Wulff, *Z. Kristallogr. Mineral.* **1901**, *34*, 449 – 530.
[17] a) D. Borthwick, V. Fiorin, S. J. Jenkins, D. A. King, *Surf. Sci.* **2008**, *602*, 2325 – 2332; b) D. C. Sorescu, *J. Phys. Chem. C* **2008**, *112*, 10472 – 10489.
[18] J. P. Perdew, K. Burke, M. Ernzerhof, *Phys. Rev. Lett.* **1996**, *77*, 3865 – 3868.
[19] P. E. Blöchl, *Phys. Rev. B* **1994**, *50*, 17953 – 17979.
[20] a) G. Kresse, J. Hafner, *Phys. Rev. B* **1993**, *48*, 13115 – 13118; b) G. Kresse, J. Furthmüller, *Phys. Rev. B* **1996**, *54*, 11169 – 11186.

 © 2011 Wiley-VCH Verlag GmbH & Co. KGaA, Weinheim